RESEARCH ARTICLE | DECEMBER 10 2024

In situ etching of *β*-Ga_2O_3 using *tert*-butyl chloride in an MOCVD system

Cameron A. Gorsak ; Henry J. Bowman ; Katie R. Gann ; Joshua T. Buontempo ; Kathleen T. Smith ; Pushpanshu Tripathi ; Jacob Steele ; Debdeep Jena ; Darrell G. Schlom ; Huili Grace Xing ; Michael O. Thompson ; Hari P. Nair

Appl. Phys. Lett. 125, 242103 (2024)
https://doi.org/10.1063/5.0239152
CHORUS

Applied Physics Letters ARTICLE pubs.aip.org/aip/apl

In situ etching of β-Ga_2O_3 using *tert*-butyl chloride in an MOCVD system

Cite as: Appl. Phys. Lett. **125**, 242103 (2024); doi: 10.1063/5.0239152
Submitted: 17 September 2024 · Accepted: 27 November 2024 ·
Published Online: 10 December 2024

Cameron A. Gorsak,[1] Henry J. Bowman,[2] Katie R. Gann,[1] Joshua T. Buontempo,[1] Kathleen T. Smith,[3] Pushpanshu Tripathi,[1] Jacob Steele,[1] Debdeep Jena,[1,4,5] Darrell G. Schlom,[1,5,6] Huili Grace Xing,[1,4,5] Michael O. Thompson,[1] and Hari P. Nair[1,a)]

AFFILIATIONS

[1]Department of Materials Science and Engineering, Cornell University, Ithaca, New York 14853, USA
[2]PARADIM REU, Cornell University, Ithaca, New York 14853, USA
[3]School of Applied and Engineering Physics, Cornell University, Ithaca, New York 14853, USA
[4]School of Electrical and Computer Engineering, Cornell University, Ithaca, New York 14853, USA
[5]Kavli Institute at Cornell for Nanoscale Science, Cornell University, Ithaca, New York 14853, USA
[6]Leibniz-Institut für Kristallzüchtung, Max-Born-Str. 2, 12489 Berlin, Germany

[a)]**Author to whom correspondence should be addressed:** hn277@cornell.edu

ABSTRACT

In this study, we investigate *in situ* etching of β-Ga_2O_3 in a metalorganic chemical vapor deposition system using *tert*-butyl chloride (TBCl). We report etching of both heteroepitaxial $(\bar{2}01)$-oriented and homoepitaxial (010)-oriented β-Ga_2O_3 films over a wide range of substrate temperatures, TBCl molar flows, and reactor pressures. We infer that the likely etchant is HCl (g), formed by the pyrolysis of TBCl in the hydrodynamic boundary layer above the substrate. The temperature dependence of the etch rate reveals two distinct regimes characterized by markedly different apparent activation energies. The extracted apparent activation energies suggest that at temperatures below ~800 °C, the etch rate is likely limited by desorption of etch products. The relative etch rates of heteroepitaxial $(\bar{2}01)$ and homoepitaxial (010) β-Ga_2O_3 were observed to scale by the ratio of the surface energies, indicating an anisotropic etch. Relatively smooth post-etch surface morphology was achieved by tuning the etching parameters for (010) homoepitaxial films.

The ultra-wide bandgap semiconductor β-Ga_2O_3 (~4.8 eV) has garnered attention recently as a platform for power electronics and radio frequency devices.[1] The ultra-wide bandgap results in a high critical breakdown field strength yielding a superior Baliga's figure of merit relative to semiconductors like SiC and GaN.[2] Progress in β-Ga_2O_3 research has been spurred by the availability of large-area (up to 4 in.) melt-grown substrates[3] and the ease of *n*-type doping.[4] Metalorganic chemical vapor deposition (MOCVD) has emerged as a technique capable of producing high-quality β-Ga_2O_3 thin films with room-temperature electron mobilities approaching the polar optical phonon limit.[5–8] A low-damage *in situ* etch to minimize contamination or plasma-induced damage before subsequent deposition of n+ material[9] or dielectrics[10] will be key for enabling higher-performance devices. In this study, we investigate the use of *tert*-butyl chloride (TBCl) as a precursor for *in situ* etching of β-Ga_2O_3.

In situ etching of β-Ga_2O_3 has been demonstrated using a flux of elemental gallium in molecular beam epitaxy (MBE) and using triethylgallium in MOCVD.[11,12] The etch mechanism for both leverages the formation of volatile gallium suboxides.[13] The use of elemental Ga can, however, potentially leave gallium metal droplets on the surface necessitating an *ex situ* HCl wet etch. Agnitron Technologies has demonstrated that these Ga droplets can be removed *in situ* with TBCl etching; however, their use of TBCl for etching of β-Ga_2O_3 itself was not promising, requiring much higher TBCl molar flow compared to those used in this work to achieve appreciable etch rates.[14] *In situ* etching of β-Ga_2O_3 has also been demonstrated in halide vapor phase epitaxy (HVPE) systems using HCl gas.[15,16]

TBCl is an attractive choice as an etchant precursor since it is relatively noncorrosive compared to HCl, displays long-term stability at room temperature, has a reasonable vapor pressure, and can be

installed in the typical bubblers, widely used for precursor delivery in MOCVD systems. *In situ* etching using TBCl has been demonstrated for various III–V semiconductors.[17–21] The thermal decomposition of TBCl has been experimentally confirmed to follow[22–24]

$$(CH_3)_3CCl(g) \rightarrow iso\text{–}C_4H_8(g) + HCl(g). \quad (1)$$

In situ etching of β-Ga_2O_3 was performed in a cold-wall Agnitron Agilis 100 MOCVD system equipped with a remote-injection showerhead. The SiC-coated graphite susceptor was inductively heated, and the substrate temperature was measured by a pyrometer aimed at the backside. The etching studies were carried out over reactor pressures of 10–60 Torr, susceptor temperatures of 700–1000 °C, and TBCl molar flows of ~20–61 μmol/min. The stainless-steel bubbler containing the TBCl (99.9999%) was purchased from Dockweiler Chemicals and was held at a pressure of 900 Torr and a temperature of 5 °C. Both heteroepitaxial $(\bar{2}01)$ β-Ga_2O_3, grown on c-plane sapphire, and homoepitaxial films, grown on Fe-doped (010) β-Ga_2O_3 from Novel Crystal Technologies, were etched. For homoepitaxial films, etching was studied at 15 and 30 Torr, 750 and 875 °C, and a TBCl molar flow of ~61 μmol/min. During etching, the total flow in the reactor was fixed at 6000 sccm using Ar (99.999%) carrier gas.

UV-vis optical reflectometry was used to measure heteroepitaxial film thickness, while x-ray diffraction (XRD) (PANalytical Empyrean) was used to determine homoepitaxial film thickness. Homoepitaxial films grown for determining the etch rate included a thin (~10 nm) β-$(Al_{0.07}Ga_{0.93})_2O_3$ interface followed by 200–300 nm of β-Ga_2O_3 which provided an index contrast resulting in Laue oscillations.[25] Atomic force microscopy (AFM) was used to evaluate the surface morphology.

We used heteroepitaxial β-Ga_2O_3 to map out the etch rate as a function of TBCl molar flow at temperatures between 700 and 900 °C (Fig. 1). At a fixed reactor pressure of 15 Torr, we found that etch rate increases linearly with TBCl molar flows between ~20 and 61 μmol/min, which enables fine control of the etch rate.

In general, the etch rate increases with increasing temperature; however, the slope of the etch rate vs TBCl molar flow jumps sharply from 800 to 850 °C, indicative of a sudden change in the etch-limiting step. At a fixed TBCl molar flow of ~61 μmol/min, the etch rate follows an Arrhenius relationship (Fig. 2). There are two distinct activation energy regimes that are commonly observed in CVD growth[26] and etching[27] processes. In our work, the low-temperature (LT) regime below ~800 °C has a higher apparent activation energy of ~1.59 and ~1.75 eV for 15 and 30 Torr, respectively. The high temperature (HT) regime above ~800 °C exhibits a much lower apparent activation energy of ~0.11 and ~0.04 eV for 15 and 30 Torr, respectively. These values are much lower than the Ga-O bond dissociation energy (~3.88 eV),[28] and we confirmed that even at the highest etch temperature employed, there is negligible thermal decomposition of β-Ga_2O_3.[29]

During the etching process, the etchant adsorbs on the surface and then reacts to form an etch product, followed by the desorption of the etch product from the surface. Based on the data from Tsang,[24] at temperatures between 700 and 1000 °C used in our work and estimated residence times[30] for precursors in the heated boundary layer above the susceptor, TBCl pyrolyzes into isobutene and hydrogen chloride (HCl) (Fig. 3). This temperature range, however, is not high enough to enable further gas-phase pyrolysis of HCl (Fig. 3).[31] Therefore, it is reasonable to assume that HCl is the etchant.

We hypothesize that the HCl adsorbs onto the surface of the β-Ga_2O_3 and reacts to form a volatile $GaCl_n$ ($n \leq 3$) etch product by one of the following three reactions, which were determined to be thermodynamically favorable based on thermochemical data[32–34] and the partial pressures of the various species at experimental conditions used in this work:

$$Ga_2O_3(s) + 6HCl(g) \leftrightarrow 2GaCl(g) + 3H_2O(g) + 2Cl_2(g), \quad (2)$$

$$Ga_2O_3(s) + 6HCl(g) \leftrightarrow 2GaCl_2(g) + 3H_2O(g) + Cl_2(g), \quad (3)$$

$$Ga_2O_3(s) + 6HCl(g) \leftrightarrow 2GaCl_3(g) + 3H_2O(g). \quad (4)$$

In the LT regime, the weak dependence of etch rate on TBCl molar flow (Fig. 1) suggests that the etch is limited by etch product desorption—either $GaCl_n$ or H_2O. While all thermodynamically favorable

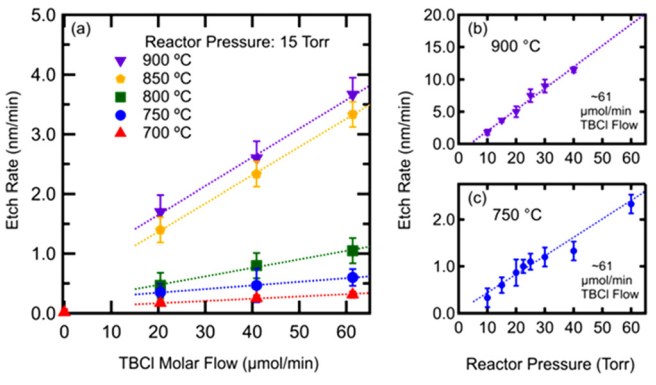

FIG. 1. Etch rate of heteroepitaxial β-Ga_2O_3 as a function of (a) TBCl molar flow and (b-c) reactor pressure. (a) At a fixed pressure of 15 Torr and temperatures between 700 and 900 °C, increasing the TBCl molar flow results in a linear increase in etch rate. At a fixed TBCl molar flow of ~61 μmol/min, the etch rate monotonically increases with reactor pressure in both the (b) HT and (c) LT regimes, indicating that TBCl etching of β-Ga_2O_3 does not occur in a mass-transport-limited regime.

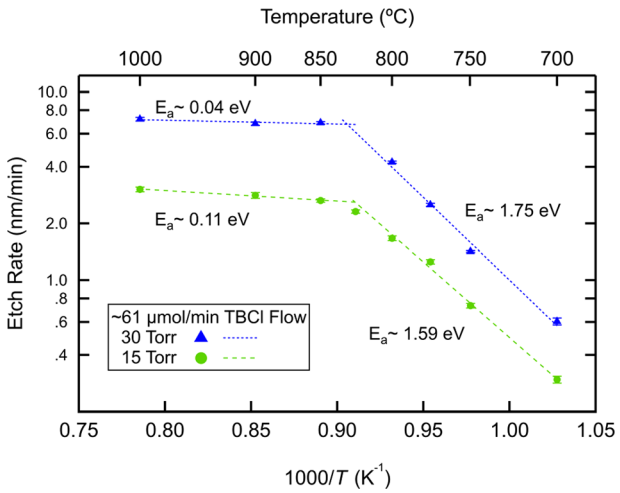

FIG. 2. Arrhenius plot of *in situ* etch rate of heteroepitaxial β-Ga_2O_3 for a TBCl molar flow of ~61 μmol/min at reactor pressures of 15 and 30 Torr. The HT and LT etch regimes are delineated by distinct apparent activation energies.

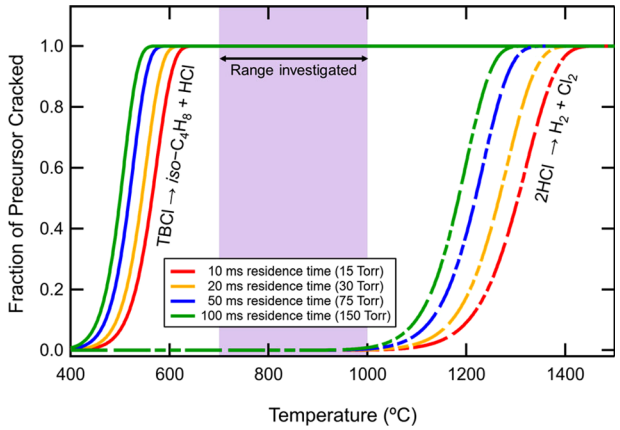

FIG. 3. Calculated fraction of TBCl and HCl pyrolyzed as a function of temperature based on typical residence times for precursors in the hot boundary layer above the substrate. The pyrolysis of TBCl into isobutene and hydrogen chloride (HCl) is fully complete by 600 °C, while the thermal decomposition of HCl does not occur until over 1000 °C.

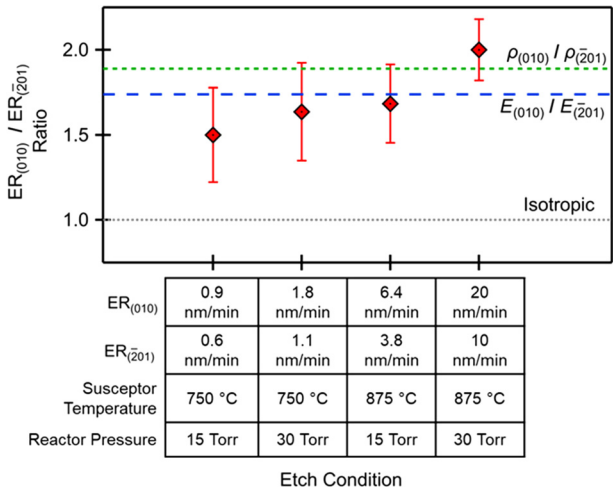

$ER_{(010)}$	0.9 nm/min	1.8 nm/min	6.4 nm/min	20 nm/min
$ER_{(\bar{2}01)}$	0.6 nm/min	1.1 nm/min	3.8 nm/min	10 nm/min
Susceptor Temperature	750 °C	750 °C	875 °C	875 °C
Reactor Pressure	15 Torr	30 Torr	15 Torr	30 Torr

FIG. 5. Comparison of etch rate between homoepitaxial (010) and heteroepitaxial $(\bar{2}01)$ β-Ga_2O_3 with ~61 μmol/min TBCl. Included in the plot are the ratios of calculated β-Ga_2O_3 dangling bond densities (ρ, green) and surface energies (E, blue) from Mu *et al.*, illustrating that the anisotropy of the etch rate is correlated with the surface energy anisotropy: the higher the surface energy, the higher the etch rate.

gas-phase reactions can occur simultaneously, $GaCl_3$ formation kinetics will depend on the surface coverage of HCl, which is likely low given the linear (first order) increase in etch rate with TBCl partial pressure, and the high vapor pressure of HCl even at 700 °C.[35,36] Therefore, the LT etch product is likely GaCl. Surface science studies of $GaCl_n$ desorption from GaAs have shown an apparent activation energy for the desorption of $GaCl_3$ and GaCl of ~0.78 and ~1.65 eV,[37] respectively.[38] When the apparent activation energy is greater than that expected for the relevant $GaCl_n$ species, the limiting factor has been attributed to the anionic species (N for GaN and As for GaAs).[39,40] For the case of β-Ga_2O_3, after the desorption of volatile $GaCl_n$ species, the surface is likely left hydroxylated. The hydroxyl-terminated β-Ga_2O_3 surface is observed to be stable up to 750 °C in an ultra-high vacuum (UHV) environment.[41] Although the activation energy for the desorption of H_2O from hydroxylated β-Ga_2O_3 is unknown at this time, the apparent activation energy for the desorption of H_2O from α-Al_2O_3 surfaces is in the range of ~1.37 to 1.78 eV, which is similar to our observations in the LT regime.[42,43] Further studies are required to fully elucidate the LT etch mechanism.

In the HT regime, the dominant $GaCl_n$ species is presumably GaCl based on thermodynamic calculations of gas-phase HVPE growth of GaN.[44] The low apparent activation energy in the HT regime agrees with the apparent activation energy (~0.08 eV) extracted above 800 °C from atmospheric pressure HCl etching of β-Ga_2O_3.[15] The etch rate in the HT regime is determined by the surface concentration of HCl as evidenced by the linear dependence of the etch rate on reactor pressure in Fig. 1(b).[45]

At high substrate temperatures, MOCVD growth typically occurs in a mass-transport-limited regime. In the absence of significant gas-phase parasitic reactions, and when all the flows are held constant, the growth rate is independent of total reactor pressure within this mass-transport-limited regime.[30,46] To determine whether etching with TBCl occurs in a mass-transport-regime, the pressure dependence of the etch rate was explored at a fixed TBCl flow rate at two temperatures: 750 °C (LT regime) and 900 °C (HT regime). The reactor pressure was controlled, independent of the total gas flow, using a computer-controlled butterfly valve in the exhaust manifold. Figures 1(b) and 1(c) show that the etch rate is increasing, and not saturating, with increasing reactor pressure, indicating that etching is not occurring in a mass-transport-limited regime even at the highest

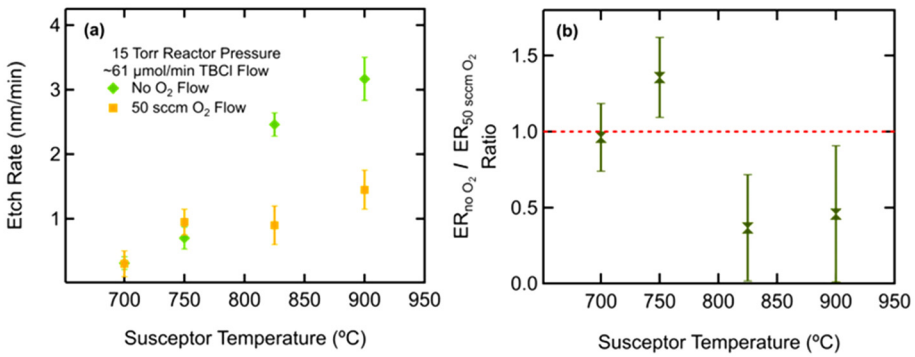

FIG. 4. Effect of additional O_2 flow on the etch rate. (a) Etch rate as a function of susceptor temperature with no O_2 (green) and with 50 sccm O_2 flow (yellow). (b) Ratio of the etch rate without oxygen divided by the etch rate with oxygen vs susceptor temperature. Below 800 °C, the etch rate is relatively unchanged, but it is suppressed at higher temperatures.

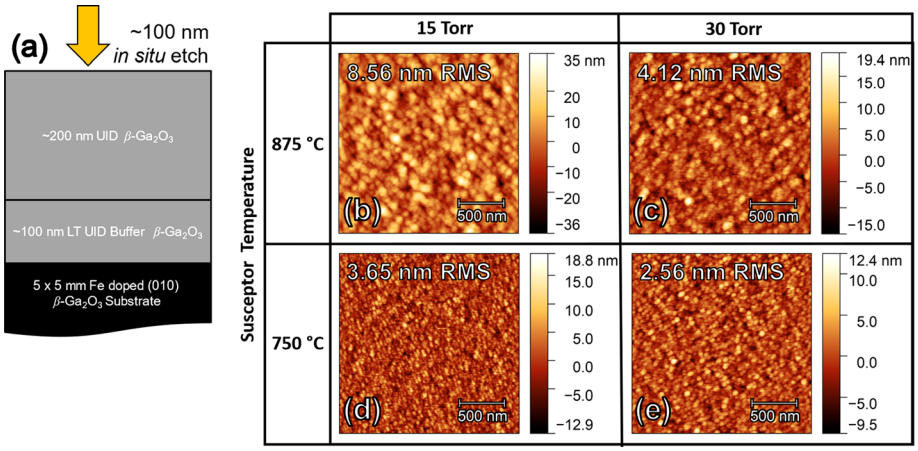

FIG. 6. Surface morphologies of *in situ* TBCl etched β-Ga_2O_3. (a) Layer structure illustrating ~100 nm *in situ* etch after growth of ~400 nm of UID β-Ga_2O_3 on Fe-doped (010) substrates. (b)–(e) AFM of surfaces after etching with ~61 μmol/min TBCl molar flow at various conditions. The 750 °C etch (bottom row) is smoother than that at 875 °C (top row). 30 Torr etching (right column) is smoother than the 15 Torr (left column).

substrate temperatures investigated in this study. An increase in etch rate with reactor pressure is likely due to the increased surface coverage of the etchant, HCl, with increasing HCl partial pressure.[45]

In order to investigate the effect of oxygen on the etch rate, we introduced a 50 sccm flow of O_2 into the reactor during etching. In the LT regime, the etch rate was largely not affected; however, in the HT regime, the etch rate was suppressed by a factor of ~2 as seen in Fig. 4. We believe that the HT etch rate is suppressed due to the competing HVPE growth back reaction.

Next, we etched co-loaded heteroepitaxial $(\bar{2}01)$ and homoepitaxial (010) β-Ga_2O_3 samples to investigate the etch rate anisotropy. The etch rate for homoepitaxial samples with ~61 μmol/min TBCl molar flow was determined by XRD (Fig. S1) for four distinct conditions (15 Torr at 750 and 875 °C, and 30 Torr at 750 and 875 °C). Figure 5 summarizes these etch rates, revealing the anisotropy. Also plotted in Fig. 5 are the ratios between the calculated (010) and $(\bar{2}01)$ dangling bond densities (ρ, green) and surface energies (E, blue), which agrees well with the experimental data.[47] Etch rate anisotropy has also been observed during etching of β-Ga_2O_3 using HCl in an HVPE reactor.[15]

To investigate the surface morphology resulting from TBCl etching, ~400 nm thick homoepitaxial (010) unintentionally doped (UID) β-Ga_2O_3 samples were grown and then immediately *in situ* etched, without cooling down, to a depth of ~100 nm for each of the four conditions shown in Figs. 6(b)–6(e). The resulting surface morphology resembles that resulting from hot phosphoric wet etching[48] and does not exhibit characteristic faceting of the (110) plane along the [001] direction typically seen post-growth[49] [as shown for an unetched film in Fig. S1(b)] or after elemental Ga etching.[11,12] In general, we observe that etching under higher pressures and low temperatures results in smoother surfaces. Currently, the exact mechanism for surface roughening is unclear, but we note that conditions for smoother etch morphologies also result in longer surface residence time of gas-phase species. We note that heteroepitaxial $(\bar{2}01)$ oriented β-Ga_2O_3 films grown on c-plane sapphire also exhibited increased surface roughness after etching using TBCl (Fig. S2).

The electrical properties are not compromised for films grown after a 30 min *ex situ* 48% hydrofluoric acid etch plus a ~50 nm *in situ*, ~61 μmol TBCl etch at 750 °C. (010) homoepitaxial films doped[50] to ~1×10^{17} and ~2×10^{18} cm^{-3} exhibit mobilities of ~115 and ~102 $cm^2/V\,s$, respectively. We demonstrate that subsequent regrowth after *in situ* etching of the substrate results in sub-nanometer RMS roughness (Fig. S3). The surface morphology of regrowth after *in situ* etching homoepitaxial films is comparable (~1 nm RMS) and is the subject of future work.

In summary, this study investigated the *in situ* etching of both heteroepitaxial $(\bar{2}01)$ and homoepitaxial (010) β-Ga_2O_3 films by TBCl in an MOCVD system over a temperature range of 700–1000 °C, pressure of 10–60 Torr, and TBCl molar flow of ~20 to 61 μmol/min. Two distinct regimes for TBCl etching of β-Ga_2O_3 were observed. The LT regime, below ~800 °C, exhibits an apparent activation energy of ~1.59 and ~1.75 eV for 15 and 30 Torr, respectively. In the LT regime, we hypothesize that the etch rate is limited by the desorption of $GaCl_n$ or likely H_2O. In the HT regime, we hypothesize that the thermodynamically favored etch product is GaCl and the apparent activation energy is low. The relationship between the etch rate of $(\bar{2}01)$ and (010) β-Ga_2O_3 scales by the ratio of surface energies. Finally, the surface morphology of *in situ* etched homoepitaxial films was evaluated, and it was determined that the lower temperature, higher pressure etch resulted in smoother surfaces. This work lays the groundwork for utilizing *in situ* TBCl etching and regrowth to obtain low-resistance ohmic contacts and improve the performance of β-Ga_2O_3 based devices.

See the supplementary material for details on MOCVD growth conditions for the films etched in this study. Also included are the XRD results used for etch rate determination, as well as AFM images of as-grown and regrown homoepitaxial films and AFM images of an as-grown and etched heteroepitaxial film.

We acknowledge support from the AFOSR/AFRL ACCESS Center of Excellence under Award No. FA9550-18-10529. C.A.G. acknowledges support from the National Defense Science and Engineering Graduate (NDSEG) Fellowship. H.J.B. acknowledges support from the National Science Foundation (NSF) [Platform for the Accelerated Realization, Analysis and Discovery of Interface Materials (PARADIM)] under Cooperative Agreement No. DMR-1539918. We also acknowledge support from PARADIM for the use of XRD. Substrate dicing and AFM were performed at the Cornell NanoScale Facility, a member of the National Nanotechnology

Coordinated Infrastructure (NNCI), which is supported by the NSF (Grant No. NNCI-2025233).

AUTHOR DECLARATIONS

Conflict of Interest

The authors have no conflicts to disclose.

Author Contributions

Cameron A. Gorsak and Henry J. Bowman contributed equally to this paper.

Cameron A. Gorsak: Conceptualization (equal); Data curation (equal); Formal analysis (equal); Investigation (lead); Methodology (equal); Visualization (equal); Writing – original draft (equal); Writing – review & editing (equal). **Henry J. Bowman:** Data curation (equal); Formal analysis (equal); Investigation (equal); Visualization (equal); Writing – original draft (equal). **Katie R. Gann:** Formal analysis (supporting); Investigation (supporting); Writing – original draft (supporting); Writing – review & editing (supporting). **Joshua T. Buontempo:** Data curation (supporting); Writing – review & editing (supporting). **Kathleen T. Smith:** Data curation (supporting); Writing – review & editing (supporting). **Pushpanshu Tripathi:** Data curation (supporting). **Jacob Steele:** Data curation (supporting); Writing – review & editing (supporting). **Debdeep Jena:** Funding acquisition (equal); Supervision (supporting). **Darrell G. Schlom:** Funding acquisition (equal); Writing – review & editing (equal). **Huili Grace Xing:** Funding acquisition (equal); Writing – review & editing (equal). **Michael O. Thompson:** Formal analysis (supporting); Funding acquisition (lead); Supervision (equal); Writing – review & editing (equal). **Hari P. Nair:** Conceptualization (lead); Formal analysis (equal); Funding acquisition (equal); Investigation (equal); Methodology (equal); Project administration (lead); Supervision (lead); Writing – original draft (equal); Writing – review & editing (equal).

DATA AVAILABILITY

The data that support the findings of this study are available from the corresponding author upon reasonable request.

REFERENCES

[1]M. J. Tadjer, "Toward gallium oxide power electronics," Science **378**, 724–725 (2022).
[2]M. Higashiwaki, K. Sasaki, A. Kuramata, T. Masui, and S. Yamakoshi, "Development of gallium oxide power devices," Phys. Status Solidi A **211**, 21–26 (2014).
[3]A. Kuramata, K. Koshi, S. Watanabe, Y. Yamaoka, T. Masui, and S. Yamakoshi, "Bulk crystal growth of Ga_2O_3," Proc. SPIE **10533**, 105330E (2018).
[4]Y. Zhang and J. S. Speck, "Importance of shallow hydrogenic dopants and material purity of ultra-wide bandgap semiconductors for vertical power electron devices," Semicond. Sci. Technol. **35**(12), 125018 (2020).
[5]A. Bhattacharyya, C. Peterson, T. Itoh, S. Roy, J. Cooke, S. Rebollo, P. Ranga, B. Sensale-Rodriguez, and S. Krishnamoorthy, "Enhancing the electron mobility in Si-doped (010) β-Ga_2O_3 films with low-temperature buffer layers," APL Mater. **11**(2), 021110 (2023).
[6]Y. Zhang, F. Alema, A. Mauze, O. S. Koksaldi, R. Miller, A. Osinsky, and J. S. Speck, "MOCVD grown epitaxial β-Ga_2O_3 thin film with an electron mobility of 176 cm^2/V s at room temperature," APL Mater. **7**(2), 022506 (2019).
[7]L. Meng, Z. Feng, A. F. M. A. Uddin Bhuiyan, and H. Zhao, "High-mobility MOCVD β-Ga_2O_3 epitaxy with fast growth rate using trimethylgallium," Cryst. Growth Des. **22**(6), 3896–3904 (2022).
[8]N. Ma, N. Tanen, A. Verma, Z. Guo, T. Luo, H. Xing, and D. Jena, "Intrinsic electron mobility limits in β-Ga_2O_3," Appl. Phys. Lett. **109**, 212101 (2016).
[9]Z. Xia, C. Joishi, S. Krishnamoorthy, S. Bajaj, Y. Zhang, M. Brenner, S. Lodha, and S. Rajan, "Delta doped β-Ga_2O_3 field effect transistors with regrown ohmic contacts," IEEE Electron Device Lett. **39**, 568–571 (2018).
[10]N. K. Kalarickal, A. Dheenan, J. F. McGlone, S. Dhara, M. Brenner, S. A. Ringel, and S. Rajan, "Demonstration of self-aligned β-Ga_2O_3 δ-doped MOSFETs with current density >550 mA/mm," Appl. Phys. Lett. **122**, 113506 (2023).
[11]N. K. Kalarickal, A. Fiedler, S. Dhara, H.-L. Huang, A. F. M. A. U. Bhuiyan, M. W. Rahman, T. Kim, Z. Xia, Z. J. Eddine, A. Dheenan, M. Brenner, H. Zhao, J. Hwang, and S. Rajan, "Planar and three-dimensional damage-free etching of β-Ga_2O_3 using atomic gallium flux," Appl. Phys. Lett. **119**(12), 123503 (2021).
[12]A. Katta, F. Alema, W. Brand, A. Gilankar, A. Osinsky, and N. K. Kalarickal, "Demonstration of MOCVD based in situ etching of β-Ga_2O_3 using TEGa," J. Appl. Phys. **135**(7), 075705 (2024).
[13]P. Vogt, F. V. E. Hensling, K. Azizie, C. S. Chang, D. Turner, J. Park, J. P. McCandless, H. Paik, B. J. Bocklund, G. Hoffman, O. Bierwagen, D. Jena, H. G. Xing, S. Mou, D. A. Muller, S.-L. Shang, Z.-K. Liu, and D. G. Schlom, "Adsorption-controlled growth of Ga_2O_3 by suboxide molecular-beam epitaxy," APL Mater. **9**(3), 031101 (2021).
[14]Agnitron Technologies, "Excelling in the etching of gallium oxide," Compd. Semicond. Mag. **29**(6) (2023).
[15]T. Oshima and Y. Oshima, "Plasma-free dry etching of (001) β-Ga_2O_3 substrates by HCl gas," Appl. Phys. Lett. **122**(16), 162102 (2023).
[16]Y. Oshima and T. Oshima, "Effect of the temperature and HCl partial pressure on selective-area gas etching of (001) β-Ga_2O_3," Jpn. J. Appl. Phys., Part 1 **62**, 080901 (2023).
[17]M. Kondow, B. Shi, and C. W. Tu, "Chemical beam etching of GaAs using a novel precursor of tertiarybutylchloride (TBCl)," Jpn. J. Appl. Phys., Part 2 **38**, L617 (1999).
[18]M. Kondow, B. Shi, and C. W. Tu, "In situ etching using a novel precursor of tertiarybutylchloride (TBCl)," J. Cryst. Growth **209**(2), 263–266 (2000).
[19]P. Wolfram, W. Ebert, J. Kreissl, and N. Grote, "MOVPE-based in situ etching of In(GaAs)P/InP using tertiarybutylchloride," J. Cryst. Growth **221**(1), 177–182 (2000).
[20]S. Codato, R. Campi, C. Rigo, and A. Stano, "Ga-assisted in situ etching of AlGaInAs and InGaAsP multi-quantum well structures using tertiarybutylchloride," J. Cryst. Growth **282**, 7–17 (2005).
[21]B. Li, M. Nami, S. Wang, and J. Han, "In situ and selective area etching of GaN by tertiarybutylchloride (TBCl)," Appl. Phys. Lett. **115**(16), 162101 (2019).
[22]D. Brearley, G. B. Kistiakowsky, and C. H. Stauffer, "The thermal decomposition of tertiary butyl and tertiary amyl chlorides, gaseous homogeneous unimolecular reactions," J. Am. Chem. Soc. **58**(1), 43–47 (1936).
[23]D. H. R. Barton and P. F. Onyon, "The kinetics of the dehydrochlorination of substituted hydrocarbons. Part IV. The mechanism of the thermal decomposition of tert.-butyl chloride," Trans. Faraday Soc. **45**, 725–735 (1949).
[24]W. Tsang, "Thermal decomposition of some tert-butyl compounds at elevated temperatures," J. Chem. Phys. **40**, 1498–1505 (1964).
[25]T. Itoh, A. Mauze, Y. Zhang, and J. S. Speck, "Epitaxial growth of β-Ga_2O_3 on (110) substrate by plasma-assisted molecular beam epitaxy," Appl. Phys. Lett. **117**(15), 152105 (2020).
[26]M. Liehr, C. M. Greenlief, S. R. Kasi, and M. Offenberg, "Kinetics of silicon epitaxy using SiH_4 in a rapid thermal chemical vapor deposition reactor," Appl. Phys. Lett. **56**(7), 629–631 (1990).
[27]A. Rebey, A. Bchetnia, and B. El Jani, "Etching of GaAs by CCl_4 and VCl_4 in a metalorganic vapor-phase epitaxy reactor," J. Cryst. Growth. **194**(3), 286–291 (1998).
[28]W.-L. Huang, Y.-Z. Lin, S.-P. Chang, W.-C. Lai, and S.-J. Chang, "Stability-enhanced resistive random-access memory via stacked $In_xGa_{1-x}O$ by the RF sputtering method," ACS Omega **6**(16), 10691–10697 (2021).
[29]S. Lany, "Defect phase diagram for doping of Ga_2O_3," APL Mater. **6**(4), 046103 (2018).
[30]L. Hui, "Mass transport analysis of a showerhead MOCVD reactor," J. Semicond. **32**(3), 033006 (2011).
[31]G. N. Schading and P. Roth, "Thermal decomposition of HCl measured by ARAS and IR diode laser spectroscopy," Combust. Flame **99**(3–4), 467–474 (1994).

[32]*CRC Handbook of Chemistry and Physics*, edited by D. R. Lide (CRC Press, 2004), Vol. 85.
[33]J. J. Reed, "The NBS tables of chemical thermodynamic properties: Selected values for inorganic and C1 and C2 organic substances in SI units," National Institute of Standards and Technology (1989). https://doi.org/10.18434/M32124 (accessed 2024-06-21)
[34]C. Chatillon and C. Bernard, "Thermodynamic calculations in CVD growth of GaAs compounds: I. Critical assessment of the thermodynamic properties for the gaseous molecules of the Ga-Cl system," J. Cryst. Growth **71**(2), 433–449 (1985).
[35]C. Su, M. Xi, Z.-G. Dai, M. F. Vernon, and B. E. Bent, "Dry etching of GaAs with Cl_2: Correlation between the surface Cl coverage and the etching rate at steady state," Surf. Sci. **282**(3), 357–370 (1993).
[36]T. Senga, Y. Matsumi, and M. Kawasaki, "Chemical dry etching mechanisms of GaAs surface by HCl and Cl_2," J. Vac. Sci. Technol. B **14**(5), 3230–3238 (1996).
[37]C. Sasaoka, Y. K. Y. Kato, and A. U. A. Usui, "Thermal desorption of gallium-chloride adsorbed on GaAs (100)," Jpn. J. Appl. Phys., Part 2 **30**(10A), L1756 (1991).
[38]C. L. French, W. S. Balch, and J. S. Foord, "Investigations of the thermal reactions of chlorine on the GaAs (100) surface," J. Phys.: Condens. Matter **3**(S), S351 (1991).
[39]D. Fahle, T. Kruecken, M. Dauelsberg, H. Kalisch, M. Heuken, and A. Vescan, "In-situ decomposition and etching of AlN and GaN in the presence of HCl," J. Cryst. Growth **393**, 89–92 (2014).
[40]J. M. Ortion, Y. Cordier, J. Garcia, and C. Grattepain, "Temperature dependence of GaAs chemical etching using $AsCl_3$," J. Cryst. Growth **164**(1), 97–103 (1996).
[41]R. M. Gazoni, L. Carroll, J. I. Scott, S. Astley, D. A. Evans, A. J. Downard, R. J. Reeves, and M. W. Allen, "Relationship between the hydroxyl termination and band bending at $(\bar{2}01)$ β-Ga_2O_3 surfaces," Phys. Rev. B **102**(3), 035304 (2020).
[42]Z. Łodziana, J. K. Nørskov, and P. Stoltze, "The stability of the hydroxylated (0001) surface of α-Al_2O_3," J. Chem. Phys. **118**(24), 11179–11188 (2003).
[43]C. E. Nelson, J. W. Elam, M. A. Cameron, M. A. Tolbert, and S. M. George, "Desorption of H_2O from a hydroxylated single-crystal α-Al_2O_3(0001) surface," Surf. Sci. **416**(3), 341–353 (1998).
[44]W. Seifert, G. Fitzl, and E. Butter, "Study on the growth rate in VPE of GaN," J. Cryst. Growth **52**, 257–262 (1981).
[45]C. E. Nelson, J. W. Elam, M. A. Tolbert, and S. M. George, "H_2O and HCl adsorption on single crystal α-Al_2O_3(0001) at stratospheric temperatures," Appl. Surf. Sci. **171**(1), 21–33 (2001).
[46]C. H. Chen, H. Liu, D. Steigerwald, W. Imler, C. P. Kuo, M. G. Craford, M. Ludowise, S. Lester, and J. Amano, "A study of parasitic reactions between NH_3 and TMGa or TMAI," J. Electron. Mater. **25**(6), 1004–1008 (1996).
[47]S. Mu, M. Wang, H. Peelaers, and C. G. Van de Walle, "First-principles surface energies for monoclinic Ga_2O_3 and Al_2O_3 and consequences for cracking of $(Al_xGa_{1-x})_2O_3$," APL Mater. **8**(9), 091105 (2020).
[48]Y. Zhang, A. Mauze, and J. S. Speck, "Anisotropic etching of β-Ga_2O_3 using hot phosphoric acid," Appl. Phys. Lett. **115**(1), 013501 (2019).
[49]P. Mazzolini and O. Bierwagen, "Towards smooth (010) β-Ga_2O_3 films homoepitaxially grown by plasma assisted molecular beam epitaxy: The impact of substrate offcut and metal-to-oxygen flux ratio," J. Phys. D: Appl. Phys. **53**(35), 354003 (2020).
[50]T.-S. Chou, S. Bin Anooz, R. Grüneberg, K. Irmscher, N. Dropka, J. Rehm, T. T. V. Tran, W. Miller, P. Seyidov, M. Albrecht, and A. Popp, "Toward precise n-type doping control in MOVPE-grown β-Ga_2O_3 thin films by deep-learning approach," Crystals **12**(1), 8 (2021).